ISSN (Print) : 0974-6846
ISSN (Online) : 0974-5645
Indian Journal of Science and Technology, *Vol 9(31), DOI: 10.17485/ijst/2016/v9i31/97743, August 2016*

Nanofluid Flow using Buongiorno Model over a Stretching Sheet and Thermophysical Properties of Nanoliquids

Nor Ashikin Abu Bakar[1]* , Norfifah Bachok[2] and Norihan Md. Arifin[2]

[1]Institute of Mathematical Engineering, Universiti Malaysia Perlis, 02600 Arau, Perlis, Malaysia; ashikinbakar@unimap.edu.my
[2]Department of Mathematics, Institute for Mathematical Research, Universiti Putra Malaysia, 43400 UPM Serdang, Selangor, Malaysia; norfifah@upm.edu.my, norihana@upm.edu.my

Abstract

The nanofluid flow using Buongiorno model over a stretching sheet and thermophysical properties of nanoliquids is numerically studied. The transformation of the governing partial differential equations into nonlinear ordinary differential equations is done using the similarity variables. Therefore, it has been solved numerically using shooting technique. Four nanoparticles (water based fluid) are considered in this study, namely silver Ag, copper Cu, aluminium oxide or known as alumina Al_2O_3 and lastly titanium oxide or known as titania TiO_2. The numerical results obtained are the velocity profile, temperature profile, and nanoparticle concentration profile. Besides, the results of the local Nusselt number and local Sherwood number are also found. These results are then displayed graphically and argued. The flow and heat transfer performance is discussed in the presence of thermophoresis *Nt* and Brownian motion *Nb* and nanoparticle volume fraction φ. This study has shown that the stretching sheet is an unique solutions. Otherwise, when φ increases, *Nb* decreases and *Nt* decreases, the heat transfer rate increases.

Keywords: Boundary Layer, Heat Transfer, Nanofluid, Stagnation Point, Stretching Sheet

1. Introduction

Currently, the research about the flow over a stretching plate are investigated by many authors. This is because the applications such as an extrusion, lubricant and glass fiber production are very important. Other applications are wire drawing, metal spinning and hot rolling. The flow past a stretching plate was founded by[1]. Then, this study has been explored by researchers. In[2] figured out the heat transfer over a stretching sheet with permeable surface. Another studies that related to stretching surface are[3–6]. Furthermore, it is noted that[7] was the first to carry out this study in a nanofluid.

The convective heat transfer in nanofluid has been pointed out over the past few years due to the importance of nanofluid. These nanofluid was first introduced by[8], where the nanoparticles are dispersed in a based fluid. There are many types of nanoparticles that widely been used such as carbon monotubes, metals, carbides or oxides, while the example of based fluids are water, engine oil, ethylene glycol or kerosene. The nanofluid has an unique behaviour that can enhance the thermal conductivity. On the other hand, the nanofluids also been used in many area such as electronics, biomedical, food, transportation and nuclear reactor. Some of the studies that considering nanofluid are[9–11].

**Author for correspondence*

In[12] introduced nanofluid model which examine the nanofluid flow and heat transfer with the existence of nanoparticles. In[13] used this model to study the hydromagnetic flow over a permeable sheet. In[14] argued the flow past a stretching or shrinking surface. On the other hand, in[15] introduced the nanofluid model that considers the affects of both Brownian motion parameter and thermophoresis paramater. These two elements are important in nanofluids. A number of researchers have studied this model currently. In[16] studied the flow towards a permeable surface. In[17] investigated the flow over an isothermal vertical plate. Other study, In[18] explained the nanofluid flow over a vertical plate.

We extend and then elaborate the study by[14,16] represent two nanofluids model of[12,15] respectively will be used together as a combination nanofluid equation model in a co-flowing nanofluid. There are very limited study in the literature that deal with these models combination, as mentioned by[19]. We aim to study the presence of thermophoresis, Brownian motion and also the nanoparticle volume fraction. The study also covered the effect of these parameters numerically on both the flow and heat transfer over a stretching plate. As default, the shooting technique will give the results for velocity, temperature and nanoparticle concentration. The results for skin friction coefficient, local Nusselt number and local Sherwood number are also obtained. All these results are shown graphically and elaborated in detail.

2. Problem Formulation

The two-dimensional free convection boundary layer flow in the area $y > 0$, past a stretching sheet when conditions for the plane, $y = 0$ and stagnation point, $x = 0$ are considered. The flow is assumed steady, laminar and incompressible. Another assumption is the stretching velocity $U_w(x)$ is vary linearly from $x = 0$, with $U_w(x) = ax$ and $U_\infty(x) = bx$, (with a and b are both constants where $b > 0$). This assumption also true for the ambient fluid velocity $U_\infty(x)$. For stretching sheet, $a > 0$, the governing equations are as follows:

$$\frac{\partial u}{\partial x}+\frac{\partial v}{\partial y}=0, \tag{1}$$

$$u\frac{\partial u}{\partial x}+v\frac{\partial u}{\partial y}=U_\infty\frac{dU_\infty}{dx}+\frac{\mu_{nf}}{\rho_{nf}}\frac{\partial^2 u}{\partial y^2}, \tag{2}$$

$$u\frac{\partial T}{\partial x}+v\frac{\partial T}{\partial y}=\alpha_{nf}\frac{\partial^2 T}{\partial y^2}+\tau\left[D_B\frac{\partial C}{\partial y}\frac{\partial T}{\partial y}+\left(\frac{D_T}{T_\infty}\right)\left(\frac{\partial T}{\partial y}\right)^2\right], \tag{3}$$

$$u\frac{\partial C}{\partial x}+v\frac{\partial C}{\partial y}=D_B\frac{\partial^2 C}{\partial y^2}+\left(\frac{D_T}{T_\infty}\right)\frac{\partial^2 T}{\partial y^2}, \tag{4}$$

along the boundary conditions:

$$\begin{aligned}&u=U_w(x),\quad v=0,\quad T=T_w,\quad C=C_w \quad \text{at } y=0,\\ &u\to U_\infty,\quad T\to T_\infty,\quad C\to C_\infty \quad \text{as } y\to\infty,\end{aligned} \tag{5}$$

with the velocity components u in x- direction and the velocity component v in y-direction, T, T_w and T_∞ are temperature, surface temperature, ambient temperature, respectively. Parameters C, C_∞ and C_w are nanoparticle volume fraction, nanoparticle volume fraction far from the plate and nanoparticle volume fraction at the plate, respectively, thermophoretic diffusion coefficient D_T, Brownian diffusion coefficient D_B, heat capacity ratio $\tau = (\rho C_p)_s/(\rho C_p)_f$, where nanoparticle heat capacity $(\rho C_p)_s$ and fluid heat capacity $(\rho C_p)_f$. Further, α_{nf}, μ_{nf} and ρ_{nf} are the nanofluid thermal diffusivity, nanofluid viscosity and nanofluid density, respectively. These parameters are defined by[20].

$$\begin{aligned}&\alpha_{nf}=\frac{k_{nf}}{(\rho C_p)_{nf}},\quad \rho_{nf}=(1-\varphi)\rho_f+\varphi\rho_s,\quad \mu_{nf}=\frac{\mu_f}{(1-\varphi)^{2.5}},\\ &(\rho C_p)_{nf}=(1-\varphi)(\rho C_p)_f+\varphi(\rho C_p)_s,\quad \frac{k_{nf}}{k_f}=\frac{(k_s+2k_f)-2\varphi(k_f-k_s)}{(k_s+2k_f)+\varphi(k_f-k_s)}.\end{aligned} \tag{6}$$

with parameter nanoparticle volume fraction φ, nanofluid heat capacity $(\rho C_p)_{nf}$, nanofluid thermal conductivity k_{nf}, fluid thermal conductivity k_f, solids thermal conductivity k_s, fluid density ρ_f, solids density ρ_s and fluid viscosity μ_f. Following[21], the term k_{nf} is refered as spherical nanoparticles and should not be considered for other shapes. Next, subject to Equation (5), we perform the similarity solution of Equation (1) till Equation (4). The similarity transformations is introduced, see[14,16]:

$$\eta=\left(\frac{U_\infty}{v_f x}\right)^{1/2} y,\quad \psi=\left(v_f x U_\infty\right)^{1/2} f(\eta),$$
$$\theta(\eta)=\frac{T-T_\infty}{T_w-T_\infty},\quad \phi(\eta)=\frac{C-C_\infty}{C_w-C_\infty}, \tag{7}$$

with the similarity variable η and the stream function ψ, where $u=\partial\psi/\partial y$ and $v=-\partial\psi/\partial x$ that satisfies Equation (1). Equation (6) is then substituted into Equation (2) and Equation (3), the transformed equations are:

$$\frac{1}{(1-\varphi)^{2.5}\left(1-\varphi+\varphi\rho_s/\rho_f\right)}f'''+ff''-f'^2+1=0, \tag{8}$$

$$\frac{1}{\Pr}\frac{k_{nf}/k_f}{\left(1-\varphi+\varphi(\rho C_p)_s/(\rho C_p)_f\right)}\theta''+\frac{1}{2}f\theta'+Nb\phi'\theta'+Nt\theta'^2=0, \tag{9}$$

$$\phi''+\frac{1}{2}Le\,f\theta'+\frac{Nt}{Nb}\theta''=0, \tag{10}$$

along with boundary conditions (5), and hence reduced to

$$f(0)=0,\ f'(0)=\varepsilon,\ \theta(0)=1,\ \phi(0)=1,$$
$$f'(\eta)\to 1,\ \theta(\eta)\to 0,\ \phi(\eta)\to 0\quad \text{as } \eta\to\infty, \tag{11}$$

with Prandtl number $\Pr=v_f/\alpha_f$, Lewis number $Le=v_f/D_B$ and stretching/shrinking parameter ε = a / b, where ε > 0 for a stretching surface. Parameters Nb and Nt are written as

The formulas of physical quantities of interest can be written as

$$Nb=\frac{(\rho C)_p D_B(C_w-C_\infty)}{(\rho C)_f v_f},\ Nt=\frac{(\rho C)_p D_T(T_w-T_\infty)}{(\rho C)_f T_\infty v_f}. \tag{12}$$

$$C_f=\frac{\tau_w}{\rho_f U_\infty{}^2},\quad Nu_x=\frac{xq_w}{k_f(T_w-T_\infty)},\quad Sh_x=\frac{xq_m}{D_B(C_w-C_\infty)}, \tag{13}$$

Where,

$$\text{surface shear stress, } \tau_w=\mu_{nf}\left(\frac{\partial u}{\partial y}\right)_{y=0}$$
$$\text{surface heat flux, } q_w=-k_{nf}\left(\frac{\partial T}{\partial y}\right)_{y=0} \tag{14}$$
$$\text{mass heat flux, } q_m=-D_B\left(\frac{\partial C}{\partial y}\right)_{y=0}.$$

Next, Equation (7) is then substituted into Equations (13) and (14), and therefore the parameters are,

$$C_f\,\mathrm{Re}_x^{1/2}=\frac{1}{(1-\varphi)^{2.5}}f''(0),$$
$$Nu_x\,\mathrm{Re}_x^{-1/2}=-\frac{k_{nf}}{k_f}\theta'(0),$$
$$Sh_x\,\mathrm{Re}_x^{-1/2}=-\phi'(0), \tag{15}$$

where local Reynolds number $\mathrm{Re}_x=Ux/v_f$.

3. Results and Discussion

The shooting techniques are used to obtain the numerical solutions for Equation (7) to Equation (9) with the boundary conditions Equation (10). Four different nanoparticles with water based fluid are used to test the influences of *Nt*, *Nb*, φ and ε. The nanoparticles used are Ag, Cu, Al_2O_3 and TiO_2. The range of φ should be between 0 to 0.2 where φ = 0 is regular fluid[20]. Moreover, the Prandtl number Pr is 6.2. The properties values of thermophysical are shown in Table 1.

Figures 1 and 2 indicate the variations of local Nusselt number $Nu_x \,\mathrm{Re}_x^{-1/2}$ local Sherwood number $Sh_x \,\mathrm{Re}_x^{-1/2}$ *Nb* for various nanoparticles when Pr = 6.2, φ = 0.1, *Le* = 3 and *Nt* = 0.1 with ε = 1.2 for stretching case. It is clearly observed that from Figure 1, the heat transfer rate decreases as *Nb* increases while the opposite trend are found in Figure 2. As is observed, the effect of various nanoparticles only gives the small changes for heat and mass flux rates.

Table 1. Thermophysical properties of nanofluids[20]

Physical properties	Base fluid	Nanoparticles			
	Water	Ag	Cu	TiO_2	Al_2O_3
$C_p(J/kgK)$	4179	235	385	686.2	765
$\rho(kg/m^3)$	997.1	10500	8933	4250	3970
$k(W/mK)$	0.613	429	400	8.9538	40

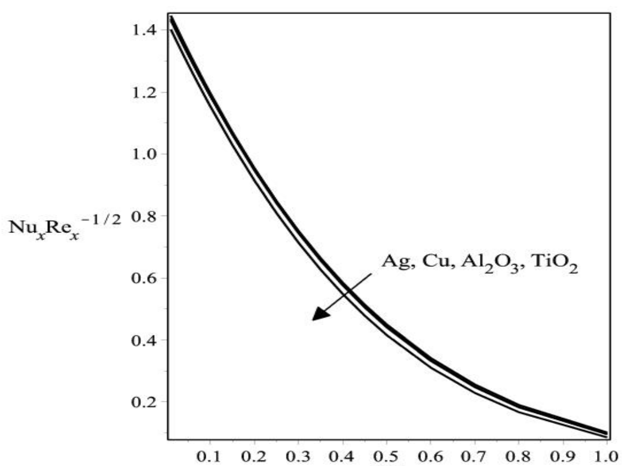

Figure 1. Variation of $Nu_x \,\mathrm{Re}_x^{-1/2}$ with Nb for various nanoparticles when ε = 1.2, Pr = 6.2, φ = 0.1, Le = 3 and Nt = 0.1.

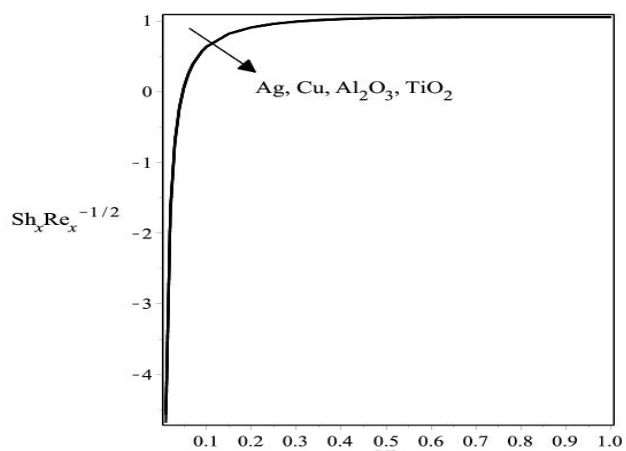

Figure 2. Variation of $Sh_x \,\mathrm{Re}_x^{-1/2}$ with Nb for various nanoparticles when ε = 1.2, Pr = 6.2, φ = 0.1, Le = 3 and Nt = 0.1.

Moreover, the variation curves of $Nu_x \mathrm{Re}_x^{-1/2}$ and $Sh_x \mathrm{Re}_x^{-1/2}$ with *Nb* for various nanoparticles when Pr = 6.2, ϕ = 0.1, *Le* = 3 and *Nt* = 0.1 with ε = 1.2 for stretching case are shown in Figure 3 ($Nu_x \mathrm{Re}_x^{-1/2}$) and Figure 4 ($Sh_x \mathrm{Re}_x^{-1/2}$). From these figures, the local Nusselt number reduces as *Nb* increases while the reverse behaviours are found in Figure 4. As is observed, the effect of various nanoparticles only give the small changes for $Nu_x \mathrm{Re}_x^{-1/2}$ and $Sh_x \mathrm{Re}_x^{-1/2}$.

Next, the variations of skin friction coefficient $C_f \mathrm{Re}_x^{1/2}$ together with $Nu_x \mathrm{Re}_x^{-1/2}$ and $Sh_x \mathrm{Re}_x^{-1/2}$ with φ for Ag, Cu, TiO_2 and Al_2O_3 when ε = 1.2 (for stretching case) with Pr=6.2, *Nt*=0.1, *Le*=3 and *Nb*=0.1 are illustrated in Figures 5, 6 and 7, respectively. It is clearly found that, for all these figures show the same trend where $C_f \mathrm{Re}_x^{1/2}$, $Nu_x \mathrm{Re}_x^{1/2}$ and $Sh_x \mathrm{Re}_x^{-1/2}$ increase when φ increases. The nanoparticle Ag is the higher value for $C_f \mathrm{Re}_x^{1/2}$ as well as $Sh_x \mathrm{Re}_x^{-1/2}$. However, nanoparticle Cu dominated the results obtained in Figure 6. The value of *f*″(0) for

Table 2. Value of f ″(0) for several values of ε when φ = 0.1

ε	*f* ″(0)			
	Ag	Cu	TiO_2	Al_2O_3
0	1.510003	1.447977	1.244317	1.231074
0.5	0.873834	0.837940	0.720083	0.712419
1	0	0	0	0
2	-2.312079	-2.217105	-1.905267	-1.884989

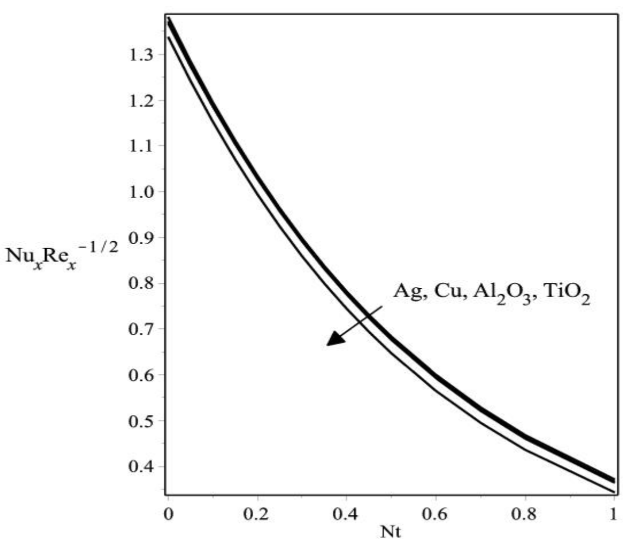

Figure 3. Variation of $Nu_x \mathrm{Re}_x^{-1/2}$ with Nt for various nanoparticles when ε = 1.2, Pr = 6.2, φ = 0.1, Le = 3 and Nb = 0.1.

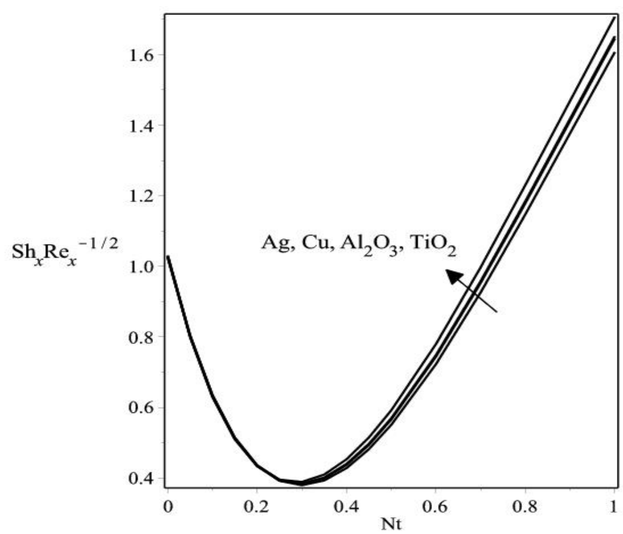

Figure 4. Variation of $Sh_x \mathrm{Re}_x^{-1/2}$ with Nt for various nanoparticles when ε = 1.2, Pr = 6.2, φ = 0.1, Le = 3 and Nb = 0.1.

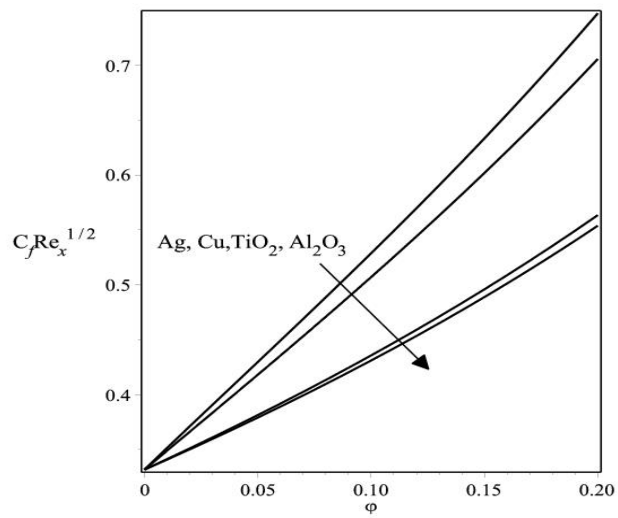

Figure 5. Variation of $C_f \operatorname{Re}_x^{1/2}$ with φ for various nanoparticles when Nb = Nt = 0.1, ε = 1.2, Pr = 6.2 and Le = 3.

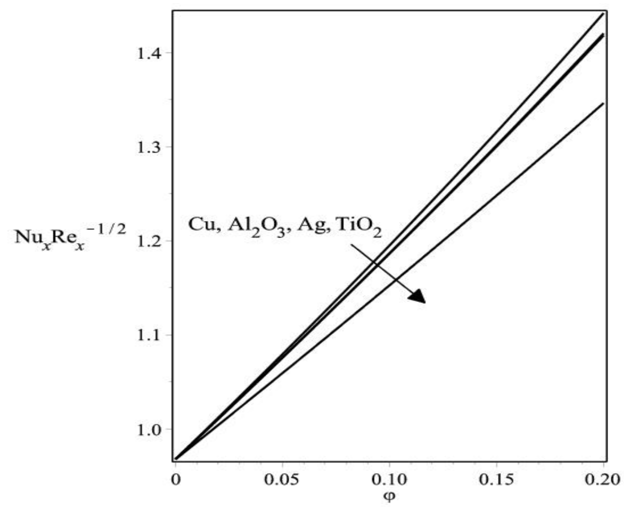

Figure 6. Variation of $Nu_x \operatorname{Re}_x^{-1/2}$ with φ for various nanoparticles when Nb = Nt = 0.1, ε = 1.2, Pr = 6.2 and Le = 3.

different ε for Ag, Cu, TiO_2 and Al_2O_3 in water when Pr = 6.2, *Nt* = 0.1, Le = 3, *Nb* = 0.1 and φ = 0.1 is shown in Table 2.

Figure 8 illustrate the changes of *Nb* on the temperature profile $\theta(\eta)$, mean while Figure 9 shows the changes of nanoparticle concentration profile $\phi(\eta)$ for Ag-water fluid when ε = 1.2, Pr = 6.2, φ = 0.1, *Le* = 3 and *Nt* = 0.1. It is noticed that a gradual increase of the temperature profile and but decreases the nanoparticle concentration profile with increasing *Nb*. Hence, in Figure 8, the boundary layer thickness increases when *Nb* increases. The opposite trend is found in Figure 9, where the boundary layer thickness reduces when *Nb* rise up. The increasing of Brownian motion is able to raise the thermal state of

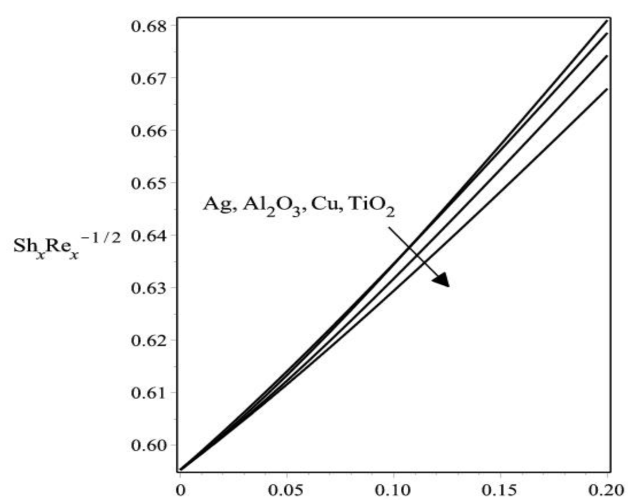

Figure 7. Variation of $Sh_x \operatorname{Re}_x^{-1/2}$ with φ for various nanoparticles when Nb = Nt = 0.1, ε = 1.2, Pr = 6.2 and Le = 3.

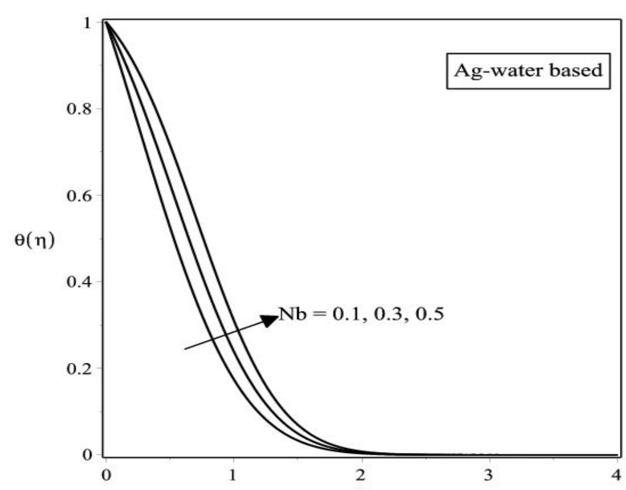

Figure 8. Temperature profile for various Nb when ε = 1.2, Pr = 6.2, φ = 0.1, Le = 3 and Nt = 0.1.

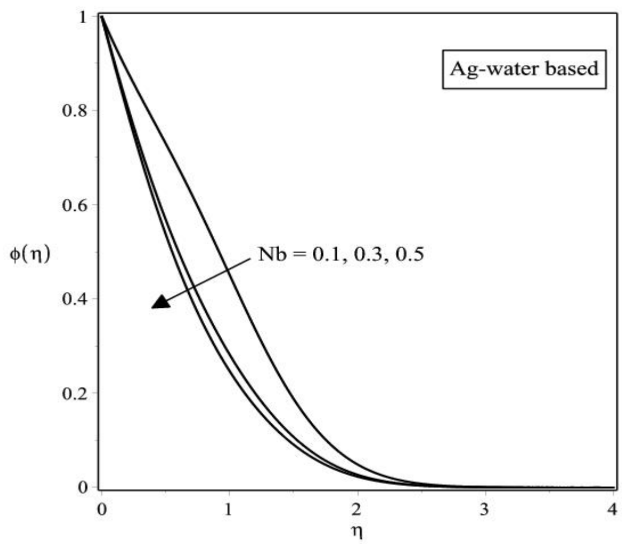

Figure 9. Concentration profile for various Nb when ε = 1.2, Pr = 6.2, φ = 0.1, Le = 3 and Nt = 0.1.

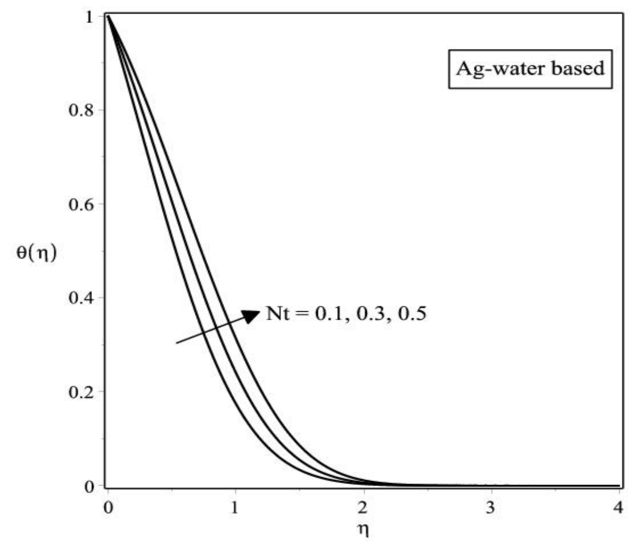

Figure 10. Temperature profile for various Nt when ε = 1.2, Pr = 6.2, φ = 0.1, Le = 3 and Nb = 0.1.

the nanofluid due to collision of the nanoparticles and based fluid.

The effects of *Nt* on θ(η) profile and ϕ(η) profile for Ag-water fluid when ε = 1.2, Pr = 6.2, φ = 0.1, *Le* = 3 and *Nb* = 0.1 are depicted in Figures 10 and 11, respectively. The figures demonstrate that θ(η) and ϕ(η) profiles increase slightly when *Nt* increases. The increasing *Nt*, the boundary layer thicknesses are more thicker. The smaller *Nt*, the thermophoresis effect blows the boundary layer thicknesses apart from the surface.

Figures 12, 13 and 14 demonstrate the effects of φ on f'(η), θ(η) and ϕ(η) profiles for Ag-water fluid when ε =

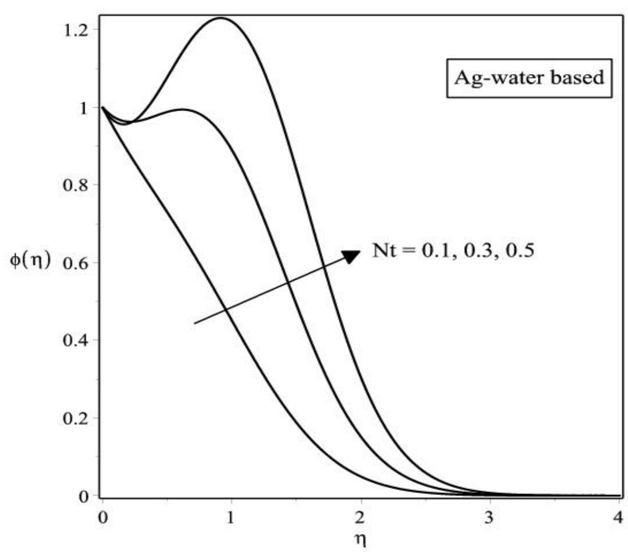

Figure 11. Concentration profile for various Nt when ε = 1.2, Pr = 6.2, φ = 0.1, Le = 3 and Nb = 0.1.

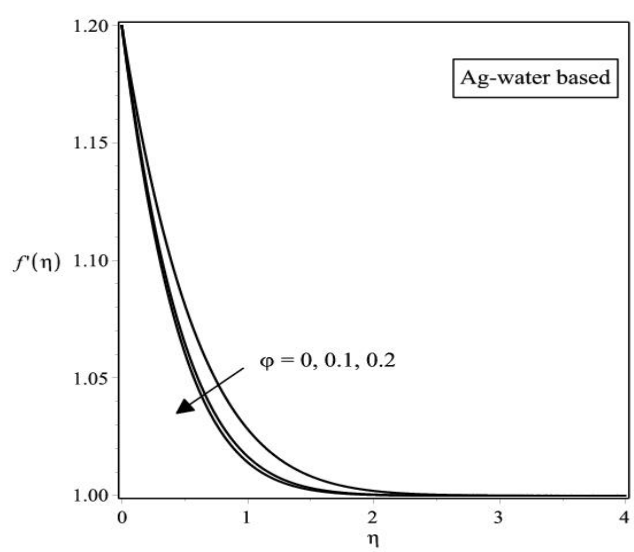

Figure 12. Velocity profile for various φ when ε = 1.2, Pr = 6.2, Le = 3 and Nb = Nt = 0.1.

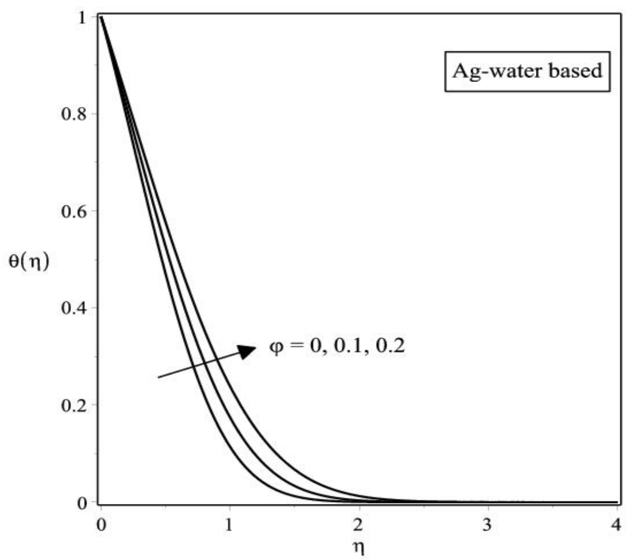

Figure 13. Temperature profile for various φ when ε = 1.2, Nt = 0.1, Pr = 6.2, Le = 3 and Nb = 0.1.

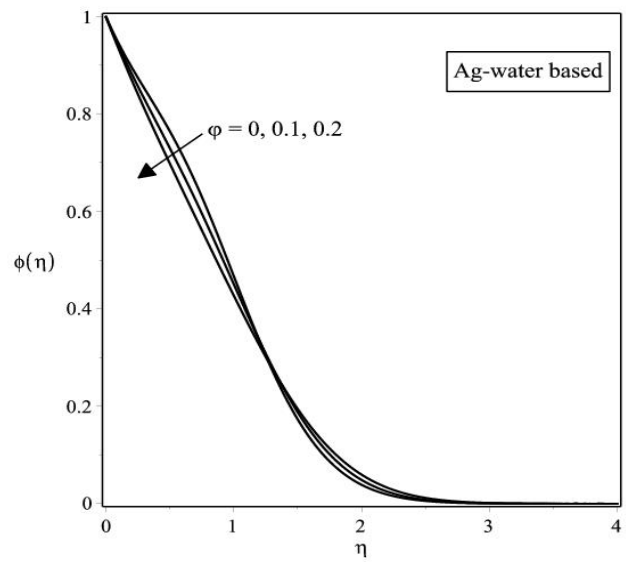

Figure 14. Concentration profile for various φ when ε = 1.2, Nt = 0.1, Pr = 6.2, Nb = 0.1 and Le = 3.

1.2, *Nb* = *Nt* = 0.1, *Le* = 3 and Pr = 6.2. From Figure 12 and Figure 14, when φ increases, $f'(\eta)$ and $\varphi(\eta)$ profiles reduce. Meanwhile in Figure 13, the reverse behaviour are found on $\theta(\eta)$ profile. The larger nanoparticle volume fraction causes the nanofluid more viscous and the mixture of convection is weaker, thus it will reduces the local Nusselt number due to high viscosity of nanofluid. The numerical results are supported because for Figure 17 till Figure 23, we found that all these profiles satisfy the boundary conditions Equation (11) asymptotically.

4. Conclusions

The nanofluid flow past a stretching sheet was examined. The influences of parameters *Nb*, *Nt*, φ and ε on, and were studied. From the investigation, an unique solution is seen for stretching sheet. Otherwise, when the φ increases, *Nb* decreases and *Nt* decreases, the heat transfer rate elevated but reduces the mass transfer rate. Besides, the heat transfer rate reduces meanwhile the mass transfer rate elevated when ε increases.

5. Acknowledgements

This research fund are supported by Universiti Putra Malaysia under Research University Grant Scheme, RUGS and also funded under Project code: FRGS/1/2015/SG 04/UPM/03/1 by Ministry of Higher Education, Malaysia. We gratefully acknowledged the financial received from them.

6. References

1. Crane LJ. Flow past a stretching plate. Z Angew Math Phys. 1970; (21):645–7.
2. Gupta PS, Gupta AS. Heat and mass transfer of a continuous stretching surface with suction or blowing. Can J Chem Eng. 1977; (55):74–6.
3. Grubka LG, Bobba KM. Heat transfer characteristics of a continuous stretching surface with variable temperature. ASME J Heat Transfer. 1985; (107):248–50.
4. Ali ME. Heat transfer characteristics of a continuous stretching surface. Warme-und Stoffubertragung. 1994; (29):227–34.

5. Wang CY. Analysis of viscous flow due to a stretching sheet with surface slip and suction. Non Analysis: Real World App. 2009; (10):375–80.
6. Hayat T, Javed T, Abbas Z. Slip flow and heat transfer of a second grade fluid past a stretching sheet through a porous space. Int J Heat and Mass Transfer. 2008; (51):4528–34.
7. Khan WA, Pop I. Boundary layer flow of a nanofluid past a stretching sheet. Int J Heat Mass Transfer. 2010; (53):2477–83.
8. Choi SUS. Enhancing thermal conductivity of fluid with nanoparticles. Proceedings, ASME International Mechanical Engineering Congress and Exposition; San Francisco, Cal, USA. ASME, FED 231/MD. 1995. p. 99–105.
9. Masuda H, Ebata A, Teramae K, Hishinuma N. Alteration of thermal conductivity and viscosity of liquid by dispersing ultra-fine particles. Netsu Bussei. 1993; (7):227–33.
10. Choi SUS, Zhang ZG, Yu W, Lockwood FE, Grulke EA. Anomalous thermal conductivity enhancement in nanotube suspensions. Applied Physics Letters. 2001; 79(14):2252–54.
11. Wang X-Q, Mumjudar AS. Heat transfer characteristics of nanofluids: A review. Int J Thermal Sci. 2007; (46):1–19.
12. Tiwari RK, Das MK. Heat transfer augmentation in a two-sided lid-driven differentially heated square cavity utilizing nanofluids. Int J Heat Mass Transfer. 2007; (50):2002–18.
13. Kameswaran PK, Narayana M, Sibanda P, Murthy PVSN. Hydromagnetic nanofluid flow due to a stretching or shrinking sheet with viscous dissipation and chemical reaction effects. Int J Heat Mass Transfer. 2012; (55):7587–95.
14. Bachok N, Ishak A, Pop I. Stagnation-point flow over a stretching/shrinking sheet in a nanofluid. Nanoscale Research Letters. 2011; (6):623–33.
15. Boungiorno J. Convective transport in nanofluids. ASME J Heat Transfer. 2006; 128: 240–50.
16. Bachok N, Ishak A, Pop I. Boundary layer stagnation-point flow toward a stretching/shrinking sheet in a nanofluid. J Heat Transfer. 2013; 135:054501.
17. Kuznetsov AV, Nield DA. Natural convective boundary layer flow of a nanofluid past a vertical plate. Int J Thermal Sci. 2010; (49):243–7.
18. Khan WA, Aziz A. Natural convection flow of a nanofluid over a vertical plate with uniform surface heat flux. Int J Thermal Sci. 2011; (50):1207–14.
19. Amin N, Nazar R, Jafar K, Pop I. Boundary-layer flow and heat transfer of nanofluids over a permeable moving surface in the presence of a coflowing fluid. Advances Mech Eng. 2014; 521236.
20. Oztop HF, Abu-Nada E. Numerical study of natural convection in partially heated rectangular enclosures filled with nanofluids. Int J Heat Fluid Flow. 2008; 29:1326–36.
21. Abu-Nada E. Application of nanofluids for heat transfer enhancement of separated flow encountered in a backward facing step. Int J Heat Fluid Flow. 2008; (29):242–9.